The Astrophysical Journal, 966:126 (10pp), 2024 May 1 https://doi.org/10.3847/1538-4357/ad307a

Enhanced Oxygen Ion Outflow at Earth and Mars due to the Concurrent Impact of a Stream Interaction Region

Indu Venugopal[1,2], Smitha V. Thampi[1], Ankush Bhaskar[1], and V. Venkataraman[1]
[1] Space Physics Laboratory, Vikram Sarabhai Space Centre, Thiruvananthapuram, 695022, India
[2] Department of Physics, Cochin University of Science and Technology, Kochi, 682022, India
Received 2024 January 11; accepted 2024 February 15; published 2024 April 30

Abstract

One of the major processes that solar wind drives is the outflow and escape of ions from the planetary atmospheres. The major ion species in the upper ionospheres of both Earth and Mars is O^+, and hence it is more likely to dominate the escape process. On Earth, due to a strong intrinsic magnetic field, the major ion outflow pathways are through the cusp, polar cap, and the auroral oval. In contrast, Mars has an induced magnetosphere, where the ionosphere is in direct contact with the shocked solar wind plasma. Therefore, physical processes underlying the ion energization and escape rates are expected to be different on Mars as compared to Earth. In the current work, we study the near-simultaneous ion outflow event from both Earth and Mars during the passage of a stream interaction region/high-speed stream (SIR/HSS) during 2016 May, when both the planets were approximately aligned on the same side of the Sun. The SIR/HSS propagation was recorded by spacecraft at the Sun–Earth L1 point and Mars Express at 1.5 au. During the passage of the SIR, the dayside and nightside ion outflows at Earth were observed by Van Allen Probes and Magnetospheric Multiscale Mission orbiters, respectively. At Mars, the ion energization at different altitudes was observed by the STATIC instrument on board the MAVEN orbiter. We observe evidence for the enhanced ion outflow from both Earth and Mars during the passage of the SIR, and identify the dominant drivers of the ion outflow.

Unified Astronomy Thesaurus concepts: Space weather (2037); Fast solar wind (1872); Planetary magnetospheres (997)

1. Introduction

Solar wind interaction can energize the ions in the upper atmosphere to higher energies, via various mechanisms, causing outflow from the planetary ionospheres. The energization of planetary ions can take place directly through the transfer of momentum or indirectly via waves, solar wind dynamic pressure, and electric fields (Jakosky et al. 2015; Schillings 2019). These processes are efficient, especially above the exobase altitude where ions have enough chance to acquire energy and escape, due to fewer collisions. In the case of both Earth and Mars, H^+ ions are continuously escaping from the planetary ionospheres as they possess enough thermal energy to escape the gravity of the planet. The next most abundant species in the upper atmospheres of both Earth and Mars is O^+. These ions require additional energization to reach the escape velocity of the planet.

Ion outflow from a planet is mainly decided by three factors: the magnetic behavior of the planet, solar wind conditions, and solar EUV flux. Of these, the magnetic behavior of the planet regulates the solar wind interaction with the planetary ionospheres, in turn controlling the ion outflow and the outflowing ions. Due to the intrinsic magnetic field of Earth, the solar wind interaction dominates in the higher latitudes or the polar regions. The direct interaction mainly occurs in the cusp region where the open magnetic fields pass through the magnetosheath region of shocked solar wind plasma (Dandouras 2021). Indirect solar wind interaction happens mainly via solar wind dynamic pressure and motional electric fields. These interactions channel down solar wind energy into the polar upper ionosphere, leading to ion outflow through various pathways; namely, the dayside cusp, polar cap, and the nightside auroral region. At equatorial latitudes of Earth, the reservoirs for plasma escape from the inner magnetosphere are the plasmasphere and the ring current (Dandouras 2021). These outflowing ions, based on their trajectory, energy, and various other factors would either remain within the planetary magnetosphere or would be lost from the planet (Dandouras 2021).

On Mars, due to the induced magnetosphere, the major ion energization mechanisms are "ion pickup" and "ion bulk escape" (Jakosky et al. 2015). In the ion pickup mechanism, ions are accelerated by the electric fields generated within the solar wind plasma penetrating the planetary ionospheres. This dominates at the altitudes <800 km (Jakosky et al. 2015). Solar wind can directly transfer momentum and strip blobs of plasma from the planetary ionosphere leading to ion bulk escape whose efficiency at Mars remains uncertain (Jakosky et al. 2015). Modeling studies have shown that for typical solar wind magnetic fields, these ions are accelerated over the poles and are lost down the wake region of the planet (Jakosky et al. 2015).

Studies have also shown that solar EUV levels have a great impact on the ion outflow process as they control the ionospheric scale height (Dandouras 2021; Nilsson et al. 2023). Transient solar events like the interplanetary coronal mass ejection (CME) and corotating interaction region (CIR) can give rise to a mixture of enhanced EUV flux levels and disturbed solar wind conditions, which can also affect the rate and density of ion outflow from the planets.

A comparative study of the magnetic behavior of the planets and space-weather phenomena offers an improved means of gaining a better understanding of the roles played by all three factors mentioned above in the atmospheric ion outflow from the planets. But, for us to compare, the two kinds of planets (magnetized and unmagnetized) must face similar space-weather conditions, including similar solar EUV flux levels. One ideal circumstance for such a study is when both the planets (magnetized and unmagnetized) are affected by the same space-weather event while they are aligned in conjunction. This ensures the similar solar EUV levels and solar wind conditions on both the planets under study (Lundin et al. 2008). However, such events are very rare. For instance, Wei et al. (2012) conducted a study of ion outflow from Earth (using the Cluster satellite) and Mars (using the Mars Express (MEX) satellite), in near conjunction during the passage of a CIR in 2008 January. Both Cluster and MEX observed enhanced ion outflow from Earth and Mars during the passage of CIR. They found that the enhanced ion outflow was triggered because of the increase in the solar wind dynamic pressure on both the planets with the Martian outflow being more sensitive to this increase. However, this study has only discussed the influence of solar wind kinetic energy on the planetary ion outflow. Other causes like the transportation of electromagnetic energy into the planetary ionospheres and particle precipitation is not covered in this study.

On 2016 May 8, Earth and Mars were in near conjunction during a similar space-weather event. The solar wind conditions of this event were previously studied by the authors Besliu-Ionescu et al. (2022) and Gruesbeck et al. (2021) and classified it as a stream interaction region/high-speed stream (SIR/HSS) event at Earth and Mars respectively. Apart from these reports on solar origin and properties, this event has not been studied in the space-weather impact perspective. In the present study, we try to understand the impact of this event on Earth and Mars, focusing on the ion outflow mechanisms. The aim is to study the outflow of O^+ ions from Earth and Mars as the origin of these ions is primarily from the planetary ionosphere rather than from solar wind, thereby making it easier to trace the outflow. Moreover, understanding the oxygen ion outflow is important because the loss of oxygen from the planetary atmospheres plays a significant role in planetary evolution (Seki et al. 2001). The conjunction (that happens every 25 months), combined with the SIR/HSS passage provides us a rare opportunity to study the effects of solar wind conditions on the ion outflow from both magnetized and unmagnetized planets.

2. Data and Methods

The Solar wind parameters at 1 minute resolution at 1 au (near the Sun–Earth L1 point) are obtained from the NASA OMNIWeb database (Papitashvili & King 2020). The measured parameters are solar wind velocity (V), density (Den.), total interplanetary magnetic field (IMF; $|B|$), the Z-component of the IMF (B_Z), the geomagnetic SYM-H index, the AL index, and the Auroral Electroject (AE) index. The solar wind parameters, i.e., solar wind velocity (V) and density (Den.) at Mars (∼1.5 au) are estimated using the Ion Mass Analyser (IMA) instrument on board the MEX orbiter while observing the unperturbed solar wind outside the bow shock region. These estimates are directly obtained from the AMDA database.[3]

The ion outflow from Earth is studied using data from the Helium Oxygen Proton Electron (HOPE; Funsten et al. 2013) mass spectrometer on board Van Allen Probe B and the Hot Plasma Composition Analyser (HPCA) of the Magnetospheric Multiscale Mission spacecraft 1 (MMS1). The HOPE mass spectrometer is a part of the Energetic particle, Composition, and Thermal Plasma (ECT) instrument on board the Van Allen Probe twin spacecraft. The Van Allen Probes orbit the Earth at a tilt of 10° with a perigee of 620 km and an apogee of 5.8 R_E (radius of the Earth). HOPE detects ions in the energy range of 1 eV q^{-1}–50 keV q^{-1}, where q is the charge of the ion, at an energy resolution of 15%. It uses the time of flight technique to identify the mass of the ions (H^+, O^+, He^+). Every 11 s, a full ion or electron measurement divided into 16 spin-angle sectors is observed (Fernandes et al. 2017). The HPCA is also a time of flight mass spectrometer, on board Magnetospheric Multiscale Mission (MMS) orbiters, designed to measure velocity distribution of H^+, O^+, He^+ in the energy range ∼10 eV–40 keV with an energy resolution ⩽20% (Young et al. 2016). The MMS orbit has an inclination of 28°, with a perigee of ∼2550 km and apogee of ∼152,900 km. The spacecraft spin is split into 32 equally spaced 11.°25 azimuthal intervals, each lasting 625 ms, to provide for an even distribution of energy and angle sampling. The ionospheric field-aligned current (FAC) development during the interval of interest is studied using the Active Magnetosphere and Planetary Electrodynamics Response Experiment[4] (AMPERE) data. AMPERE is an Earth-observing system by the US consisting of 66 spacecraft in circular polar orbits at altitudes of ∼780 km, giving near real-time magnetic field information, to obtain global maps of FACs. The data is plotted using GeospaceLAB. visualization.mpl.geomap.geodashboards, an open-source Python package to manage and visualize data in space physics (Cai et al. 2022).

The ion energization at Mars is observed using the SupraThermal And Thermal Ion Composition (STATIC) instrument of the Mars Atmosphere and Volatile Evolution (MAVEN) orbiter (McFadden 2024), which has an inclination of 75° and a periareion altitude of 150 km. The STATIC consists of a toroidal "top hat" electrostatic analyzer with a 360° × 90° field of view and a time-of-flight velocity analyzer with a 22.°5 resolution in the detecting plane. STATIC measures the composition and distribution of ions in the energy range 0.1 eV q^{-1}–30 keV q^{-1} in the mass range 1–70 amu q^{-1} (q is the charge of the ion) at 4 s resolution (McFadden et al. 2015).

3. Observations

Figure 1(a) shows the positions of the terrestrial planets on 2016 May 8. All inner planets with the exception of Venus were approximately aligned on the same side of the Sun. The Advanced Composition Explorer (ACE) and Wind at Sun–Earth L1 observed the solar wind conditions at 1 au, while MEX observed the solar wind conditions near 1.5 au. Figure 1(b) shows the orbit of IMA/MEX, which observed the pristine solar wind near 1.5 au, while MAVEN observed the region within the Martian bow shock.

The solar wind parameters at 1 au retrieved from the OMNI database are shown in Figures 2 (a)–(d) (black data points). Figures 2 (e)–(g) shows the geoeffectiveness of the event using

[3] http://amda.cdpp.eu (Automated Multi-Dataset Analysis), which is an online database and analysis software for in situ and modeled planetary plasma data.

[4] https://ampere.jhuapl.edu/products/

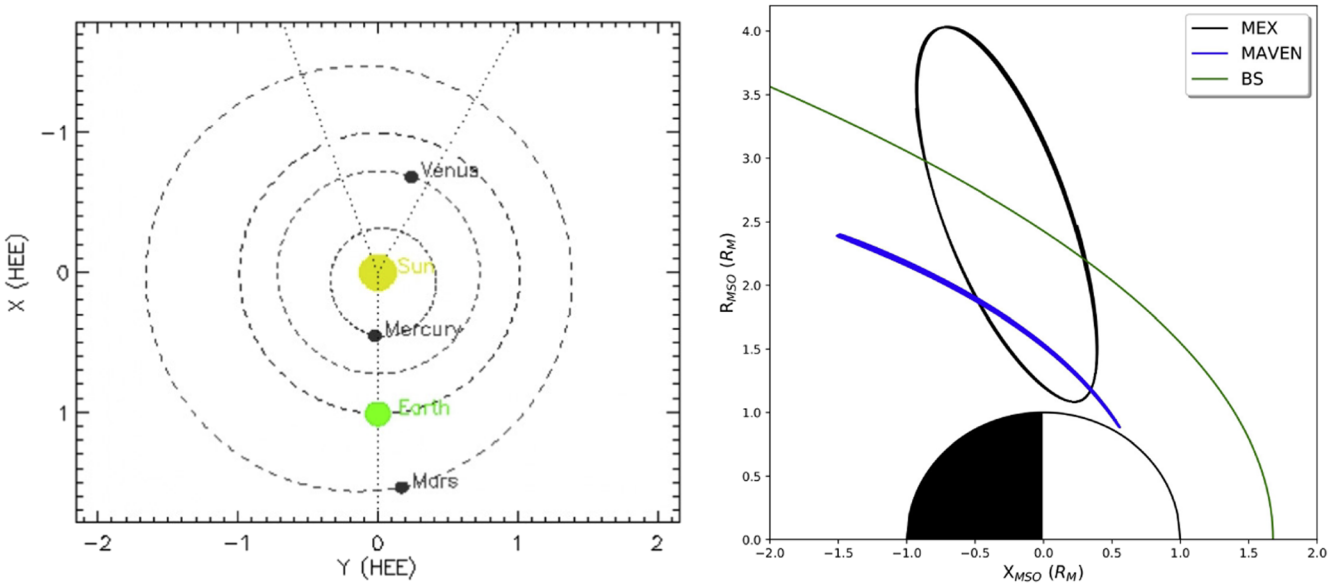

(a) (b)

Figure 1. (a) The positions of inner planets on 2016 May 8. The figure is adapted from https://stereo-ssc.nascom.nasa.gov/cgi-bin/make_where_gif. (b) The orbits of MEX and MAVEN on 2016 May 9. The bow shock location based on the analytical expression given by Hall et al. (2019) is also shown.

the Sym-H index, AL index, and AE index. It can be seen that the SIR/HSS arrived at 1 au during May 6 and was observed by WIND/ACE (Besliu-Ionescu et al. 2022). The SIR/HSS triggered a minor geomagnetic storm on Earth with a Sym-H index less than −100 nT and lasted for several days (Besliu-Ionescu et al. 2022). The arrival of SIR/HSS during May 6–7 is identified as a weak enhancement in the solar wind velocity (V), proton density (Den.), total IMF (B), and southward (B_Z) component of B (see Figure 2). After a decrease, the major enhancement happened on 2016 May 8 where the solar wind velocity increased above 600 km s^{-1}, proton density reached ∼15 cm^{-3}, which was ∼6 cm^{-3} during quiet periods, and the compressed total IMF peaked at 17 nT. On May 8 the B_Z component switched to a negative (southward) value, which coincided with a sharp decrease in the Sym-H index and AL index, and an enhancement in the AE index. Afterward, the B_Z component fluctuated between positive and negative values with a persisting low Sym-H index. The AL and AE index fluctuations reached a magnitude of ∼1800 nT, indicating strong geomagnetic storm/substorm disturbance in the auroral region.

We infer the arrival of SIR/HSS at 1.5 au from the solar wind conditions obtained from the IMA observations of the MEX orbiter shown in Figures 2 (a) and (b) (red data points). The solar wind velocity (V) started increasing slowly on May 9 peaked during May 11–12 and then gradually began to decrease. The proton density (Den.) enhancement peaked on May 9, indicating the passage of the compression region of the SIR/HSS and it persisted for 2 days (see Figure 2(b); red data points).

3.1. Ion Outflow from Earth

In this section, we describe the O^+ ion outflow from the Earth's ionosphere during the passage of SIR/HSS on 2016 May 8. Figure 3 shows the position of the Van Allen Probes A and B (RBSP A and B) and the MMS orbiters on 2016 May 8 at 04:00 UT, when the geomagnetic storm was in its main phase. The dayside ion outflow data is observed by the Van Allen Probes. Figure 4 shows the dayside ion outflow event on 2016 May 8, observed by Van Allen Probe B, where panels (a)–(c) show the O^+ ion energy-time spectrograms for pitch angles 18°, 90°, and 162° acquired by the HOPE instrument on board Van Allen Probe B and panel (d) shows the L value and the magnetic local time (MLT; right y-axis) of the spacecraft from 01:00 to 05:00 UT. The L value is the radius of the equator crossing point of a fixed field line measured in R_E.

It can be seen that from 02:15 to 04:30 UT, there is energy dispersion and an enhancement in the O^+ ion flux density, in the 18° and 162° pitch angle observations. Initially, when the Van Allen Probe B is near its apogee ($> L = 6$) we see dispersive enhancements at 162° pitch angle and as it moves toward its perigee we start seeing dispersive enhancements at 18° pitch angle as well ($< L = 6$). We do not see any enhancements in the 90° pitch angle observations. During this period of interest (02:15–04:30 UT) Van Allen Probe B is in the early morning sector. Throughout the interval, the geomagnetic storm is slowly intensifying with a decreasing SYM-H index and strong perturbations in the AL and AE indices. The nightside magnetotail region being a source of these enhanced O^+ ion fluxes is unlikely since it takes a longer time for these ions to circulate and arrive at the dayside inner magnetosphere (Liu & Zong 2022). Therefore, this indicates the possibility of a bidirectional field-aligned outflow of O^+ ions through the closed magnetic field lines, directly from high-latitude ionospheres of the dawnside polar caps of both the hemispheres. The dayside O^+ ion outflow is found to be enhanced by solar wind dynamic pressure (Fuselier et al. 2002) and further accelerated by the solar wind electric fields (Cully et al. 2003). These outflowing ions are convected toward the dayside when the B_Z component of IMF is northward and toward the nightside when the B_Z component is southward (Fuselier et al. 1989). For this event, the geomagnetic storm commences at ∼00:00 UT of May 8, with an increased northward B_Z component of IMF, before it switches

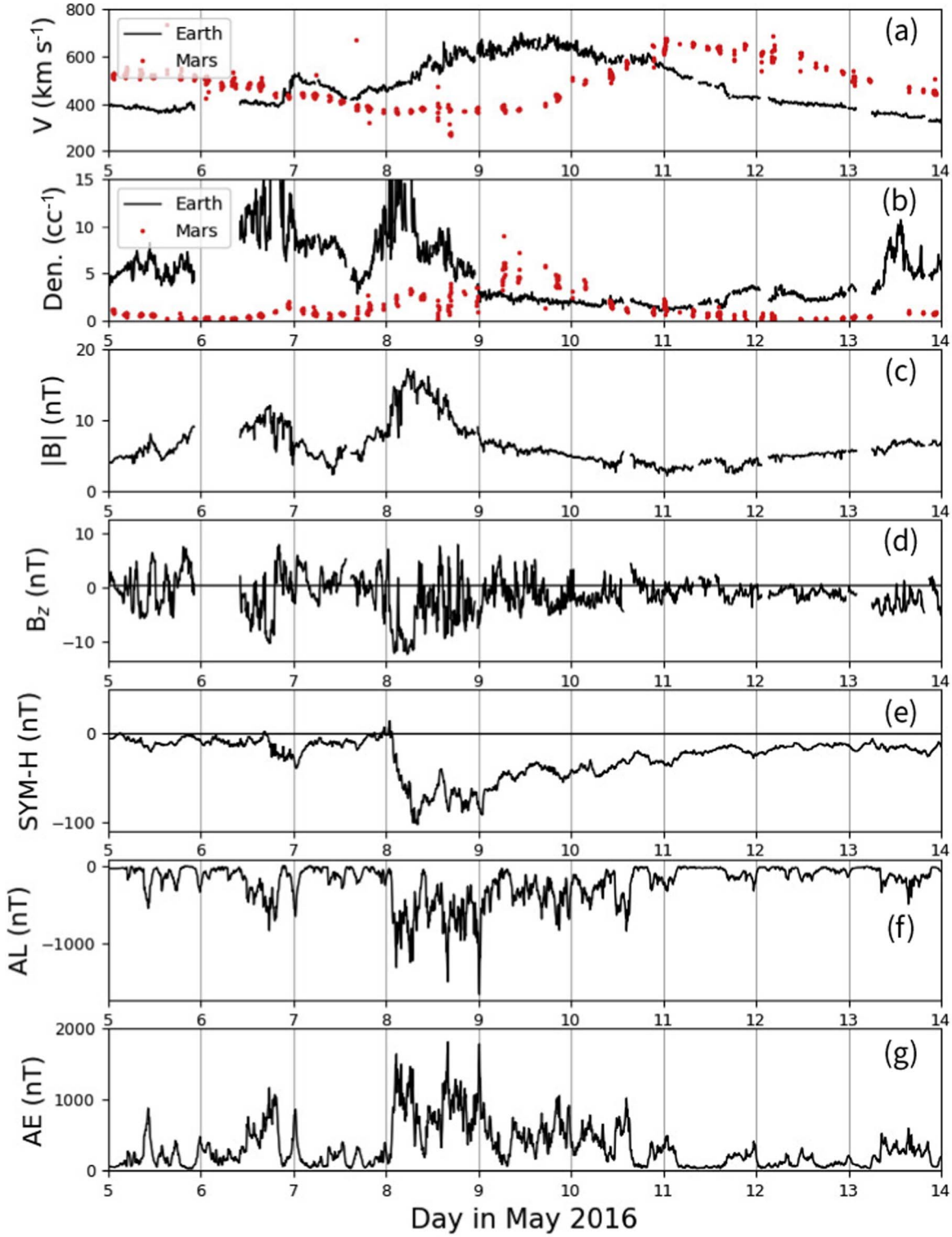

Figure 2. The temporal variations of (a) solar wind speed near Earth and Mars, (b) solar wind density near Earth and Mars, (c) magnitude of interplanetary magnetic field near Earth, (d) the *Z*-component of interplanetary magnetic field near Earth, (e) the Sym-H variation, (f) the AL index, and (g) the AE index at Earth for the period 2016 May 5–13.

southward during the main phase of the storm. This initial northward B_Z component of IMF has probably triggered the sunward convection of O^+ ions from the dawnside polar cap region and has traveled down the magnetic field lines to reach the spacecraft. The dispersive enhancements show a banded structure in both 162° and 18° pitch angle observations (see Figures 4(a)–(c)). Similar structures were previously studied by Gkioulidou et al. (2019). The observed bands in the O^+ energy-time spectrograms were attributed to the result of short-term ionospheric outflow from high-latitude ionospheres and their subsequent bounce motion along the field lines with an added $E \times B$ drift. Here only the Probe B observations are shown as the flux enhancement features are clearer in the Van Allen Probe B observations.

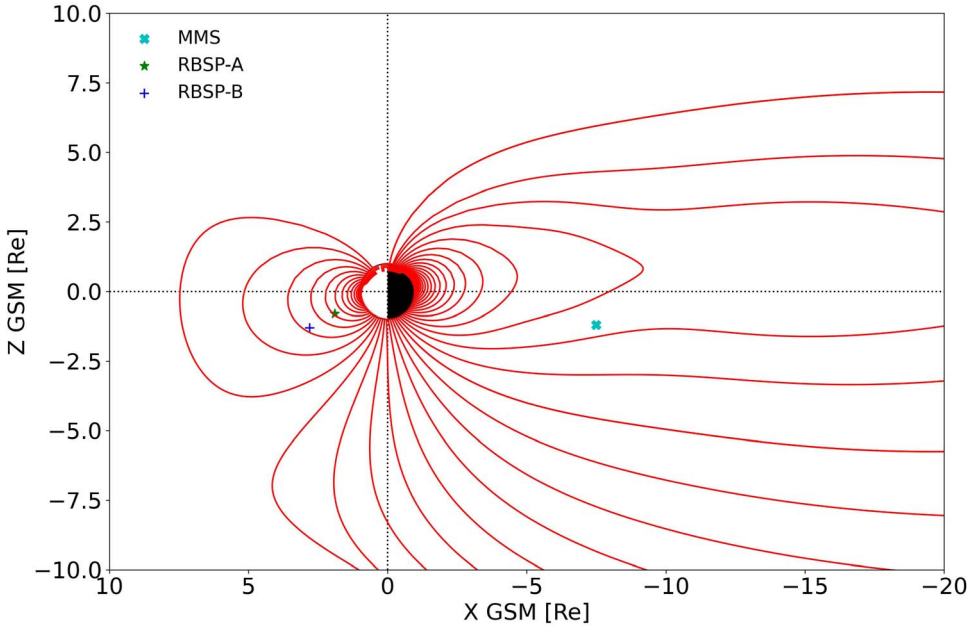

Figure 3. Position of Van Allen Probes A and B and MMS satellites on 2016 May 8 at 04:00 UT.

On May 8 the nightside ion outflow was observed by the MMS orbiters. During the period ∼00:00–12:00 UT, the MMS orbiters moved from $\sim L = 6$ to $L = 15$, after which, from ∼12:00 to 24:00 UT, they moved to a lower L value to $\sim L = 9$. Figure 5(a) shows the H^+ number density observed by HPCA on board MMS1. The high value of the H^+ number density (>1.5 cm^{-3}) is a clear indication that the spacecraft is within the plasma sheet throughout the period of observation (Kistler et al. 2019). Figure 5(b) shows the omnidirectional O^+ ion intensities observed by the HPCA instrument on board MMS1. On May 8 there was a strong increase in the O^+ flux in energies higher than 100 eV, compared to other days of the month. This energy-dispersed enhancement is attributed to the main phase of the geomagnetic storm resulted due to the passage of SIR/HSS. On the same day, the major enhancement in O^+ intensity is observed within $\sim L = 6$ and $L = 13$ in the energy range ∼0.1–6 keV (see Figure 5(b)). After this, the O^+ intensity decreases, as the spacecraft moves from $\sim L = 14$ to $L = 15$. A weak increase in intensity in energies less than 1 keV is seen when the spacecraft returned to $\sim L = 13$. During this period, from the position of the MMS satellite and the magnetic field direction, it is understood that the MMS is in the southern plasma sheet region. Therefore, the major flux enhancement we see within $\sim L = 6$–$L = 13$ could be from the outflowing O^+ ions streaming along the magnetic field from the southern polar ionosphere. The observed enhancements may be attributed to two major sources; the dayside cusp and the auroral oval (Kistler et al. 2019). These ions, outflow from the high-latitude ionospheres are convected toward the magnetotail region, and during their travel, they are found to be accelerated to energies above 1 keV due to centrifugal acceleration and $E \times B$ drift toward the plasma sheet (Kistler et al. 2019).

3.1.1. Role of Particle Precipitation in Initiating the Ionospheric Outflow

Energetic particle precipitation is found to play a major role in the topside ionospheric ion outflow. Strong upward FACs indicate electron precipitation and Joule heating, that can energize the ions from the upper ionosphere and trigger their escape (Strangeway et al. 2005; Gkioulidou et al. 2019). Therefore, to understand this phenomenon we studied the FAC evolution using AMPERE data, for the periods of enhanced ion outflows from the dayside and nightside polar regions. Figure 6 shows the AMPERE-derived FAC (upward: red; downward: blue) for three intervals of 2016 May 8. Figure 6(a) is from 00:00 to 00:10 UT corresponding to the period of storm commencement. Figures 6(b)–(c) are from 03:00–03:10 UT to 04:30–04:40 UT corresponding to the periods of observed enhanced outflows. Strong upward FACs are found in the early morning sector and throughout the night sector (see Figures 6(b)–(c)). These upward FACs indicate enhanced electron precipitation, which could be a cause for the increased O^+ ion outflow observed by the Van Allen Probe B near the dawnside and by the MMS orbiters throughout the night sector (including the cusp and the auroral region outflow).

3.2. Ion Outflow from Mars

The Martian ionosphere is found to have cold O^+ ions with energies < 10 eV, which is less than the energy required to escape the gravity of the planet (Fowler et al. 2017). Above the exobase altitude, these ions can be accelerated above the escape velocity by electric fields produced by various mechanisms (Zhang 2023). These energization mechanisms are found to become dominant during space-weather events like the passage of a CME or CIR.

In this case, as mentioned earlier, the SIR/HSS arrived at Mars on 2016 May 9 (see Figure 2). Figure 7 shows the measurements of STATIC on board the MAVEN orbiter, at two different altitudes (450 and 600) during its inbound orbit on 2016 May 5 (quiet period), 9, and 10 (event period). On May 5, the majority of the flux of all the ion species (H^+, H_2^+, O^+, and O_2^+) is found to be distributed at energies less than 10 eV at both altitudes. This indicates the presence of cold ions of ionosphere with no significant energization. After the arrival of the SIR/HSS at Mars, on May 9, an increase in light ion (H^+, He^{++}) energy spread (eV to a few keV) and flux is

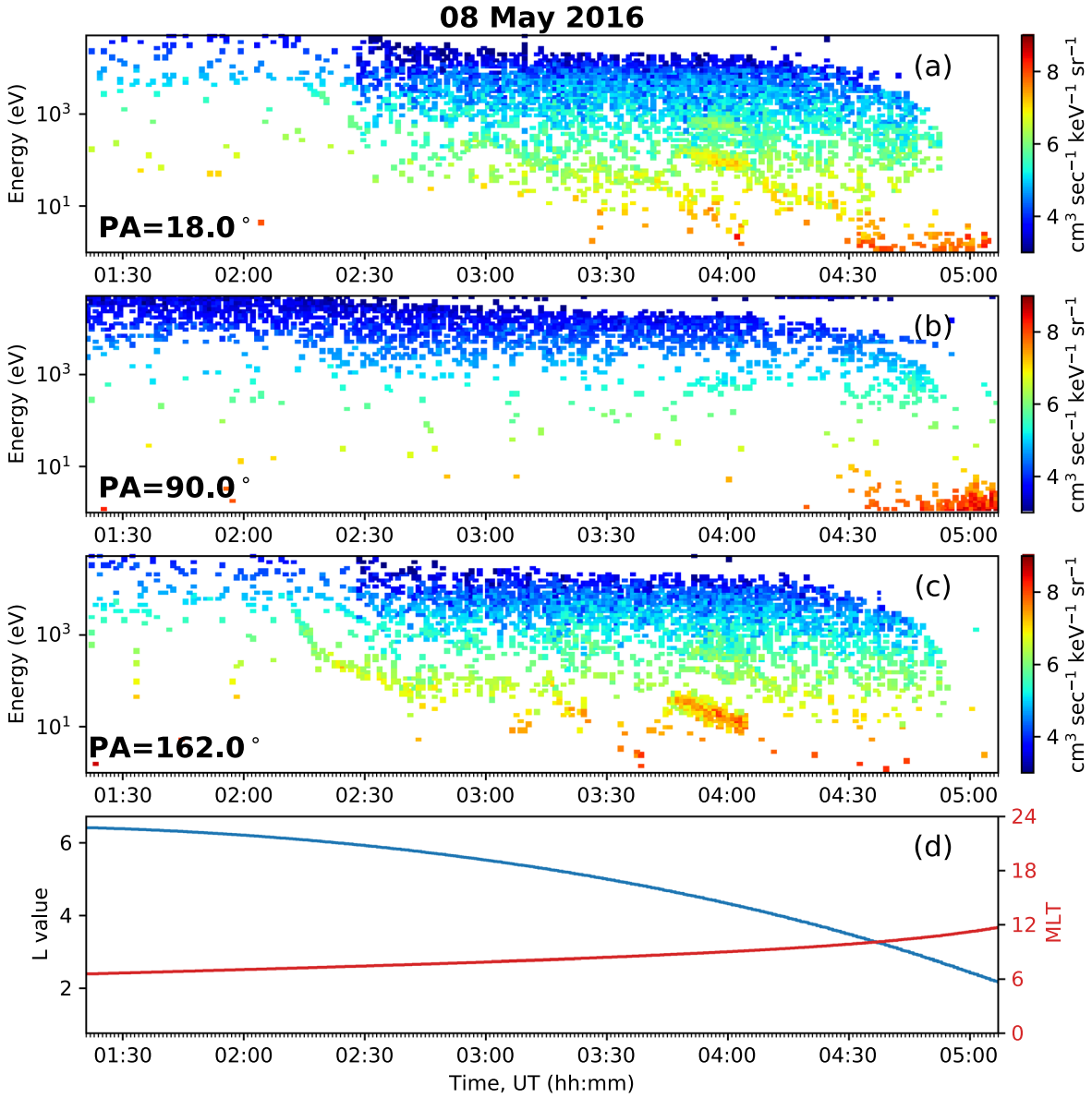

Figure 4. Van Allen Probe B HOPE energy-time spectrograms showing O^+ intensities at (a) 18°, (b) 90°, and (c) 162° pitch angles; (d) L-dipole value and MLT of the spacecraft.

observed. This enhancement in energy spread and flux becomes stronger on May 10 at both altitudes. The peak of the flux distribution of the ions is found to be shifted to higher energies at 600 km during the event periods. Previous ionospheric studies suggested that the magnetosheath and the solar wind are the two major sources of the higher-energy protons observed in the Martian upper ionosphere (Karoly 2012; Harada et al. 2015). Therefore, the spread in energy and increase in the flux indicates the deeper penetration and interaction of solar wind at these altitudes (Jakosky et al. 2015). The heavy ions (O^+ and O_2^+) are found to follow a similar trend as the lighter ions, especially the O^+ ions. Harada et al. (2015) in their study, summarized the origins of the oxygen ions of varying energies. They suggested that the cold O^+ ions (<10 eV) most likely have an ionospheric origin, while the suprathermal ions, having energies >25 eV, could be produced through ion heating by ion–ion instabilities in mixed plasma of ionosphere and solar wind. Finally, the O^+ ions having energies in keV (even higher than the solar wind) implies pickup acceleration by solar wind motional electric field (Jakosky et al. 2015). On May 10, the O_2^+ ion intensity is found to be lesser than that of the O^+ ions. This could be because of the higher scale height of the O^+ ions compared to the O_2^+ ions (Madanian et al. 2024), which again could have increased as a result of the increased dissociative recombination and charge exchange due to increased solar wind densities (Thampi et al. 2018).

4. Discussion

At Earth, on May 8, enhanced O^+ ion intensities were observed in the dayside (Van Allen Probe B) and nightside (MMS1), within a few hours of the commencement of the main phase of the geomagnetic storm. This indicates the direct injection of O^+ ions from the high-latitude ionosphere to the inner magnetosphere. In general, the upper ionospheric ions would take a longer time to reach the inner magnetosphere from the nightside tail due to usual magnetospheric convection (Liu & Zong 2022). The Van Allen Probes observed the

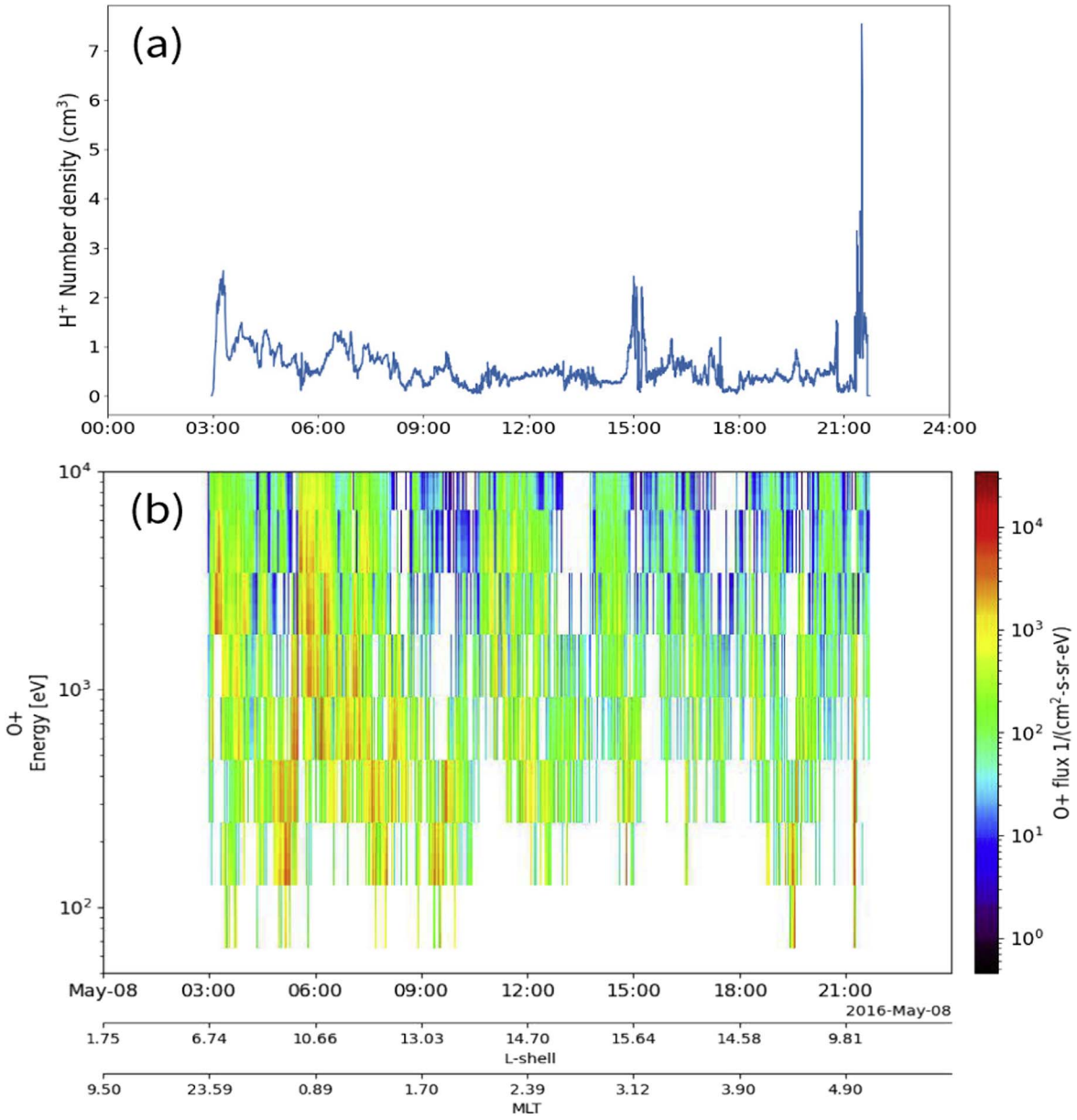

Figure 5. Data of 2016 May 8 observed by MMS1. (a) H^+ number density from MMS1. (b) O^+ omnidirectional energy flux from MMS1.

bidirectional field-aligned O^+ outflows near the dawn sector of May 8 as it moved from $L = 6$ to $L = 3$ and the source identified is the dawnside high-latitude ionosphere. Similarly, MMS orbiters observed enhanced intensities of O^+ ions from the nightside magnetotail as it moved from $\sim L = 6$ to $L = 15$ within the plasma sheet, which could be the outflowing ions from the southern polar ionosphere. The nightside ion outflow observed is mainly from the dayside cusp and the nightside auroral oval. Two potential energization mechanisms for these high-latitude ion outflows are identified. One is the solar wind dynamic pressure increase due to the arrival of the SIR/HSS (Wei et al. 2012). The second, is the electron precipitation through strong upward FAC observed near the dawn sector and throughout the night sector. Electron precipitation can energize the ions either by increasing ion scale height by ion heating or by increasing electron scale height, increasing ambipolar diffusion and acceleration of the ions (Schillings 2019). These ions could have convected to the dayside inner magnetosphere or nightside magnetotail region based on the orientation IMF B_Z (northward or southward) while the storm was progressing. Both Van Allen probes and the MMS orbiters observed a spectrum of energies in the range of eV–keV. The ions outflowing from the magnetosphere could initially be trapped within the magnetosphere, undergoing the bounce and drift motions. They also get accelerated due to mechanisms like $E \times B$ drift and centrifugal acceleration while the energization is dependent on their initial energy (Gkioulidou et al. 2019; Caggiano & Paty 2022). Therefore, we see a spectrum of energy in both dayside and nightside outflowing ions. These results are similar to the observations of the Van Allen Probes and MMS orbiters of the nightside ionospheric outflow reported by Gkioulidou et al. (2019) and Kistler et al. (2019).

We have tried to understand the O^+ ion energization from Mars well above the exobase altitude (Fowler et al. 2017) at 450 and 600 km, using the MAVEN orbiter. On May 5, i.e., well before the passage of SIR/HSS, we observe ions

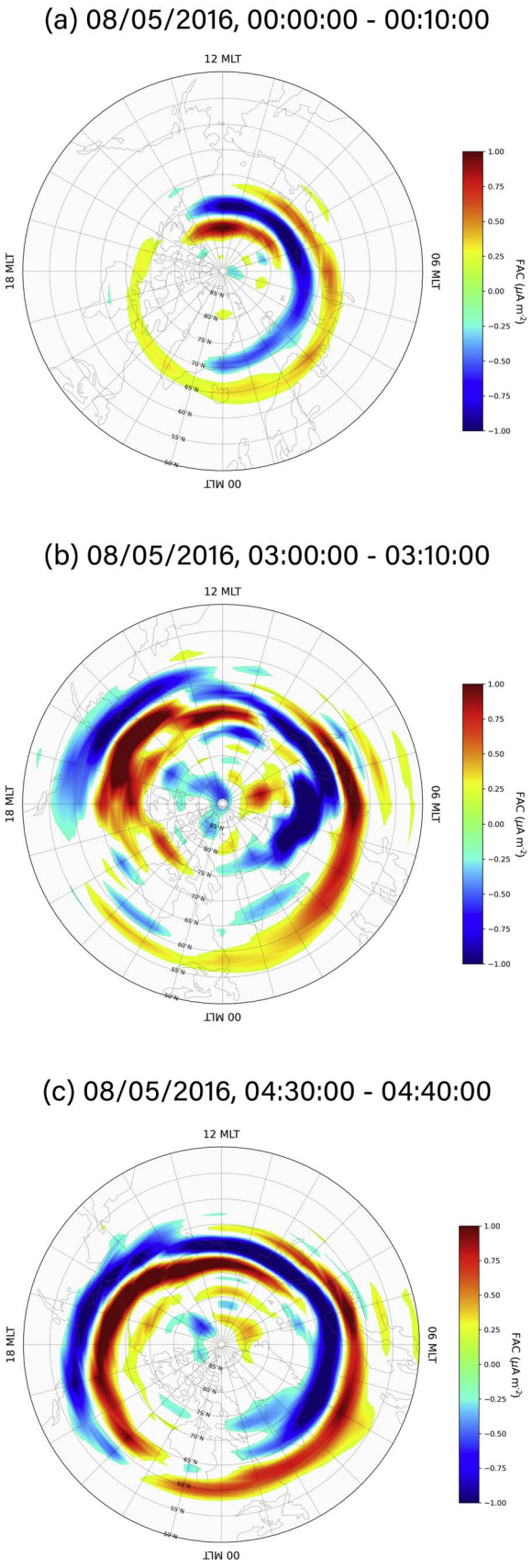

Figure 6. Maps of field-aligned currents derived from Active Magnetosphere and Planetary Electrodynamics Response Experiment (AMPERE) observations (upward: red; downward: blue) for three intervals (a) prior to and (b), (c) during the disturbance. The plots are generated using the python package GeospaceLAB (Cai et al. 2022).

essentially with thermal energies (<10 eV), basically of ionospheric origin (Lundin et al. 2006). During the event periods (May 9 and 10), a spectrum of energy is observed for both heavy and light ions at 450 and 600 km altitudes. The shielding provided by the induced magnetosphere of Mars against the solar wind is not sufficient, due to which the solar wind is seen to penetrate down to altitudes of 300 km (Lundin et al. 2006). Solar wind ions (H^+ and He^{++}) have large gyroradius, which enables them to penetrate the magnetic pileup boundary and reach the lower altitudes (Dieval 2011). Therefore, the low energy part of the light ion spectrum is from the ionospheric ions, and the energies ∼1 keV observed are of the solar wind ions. This implies the penetration of solar wind ions deeper down to altitudes of 450 km. These observations agree with the previous studies by Lundin et al. (2006) and Lundin et al. (2004). This deep penetrating solar wind could be a source of ion energization in the dayside Martian ionosphere through direct energy and momentum transfer (Lundin et al. 2004). Another major ion energization mechanism in the dayside ionosphere at this high altitude is the 'classical ion pickup' by solar wind motional electric fields and it dominates below <800 km where the solar wind velocity is high enough to accelerate the ions (Jakosky et al. 2015; Li et al. 2023). These electric fields can be produced due to the bulk motion of the magnetic field (Li et al. 2023). The heavy ions are energized to the keV range and will gyrate around the magnetic field lines with a huge gyroradius (∼30,000 km for O^+ ions) to reach higher altitudes (Jakosky et al. 2015). The suprathermal ion energies observed during May 9 and 10 for O^+ ions may be attributed to ion–ion instabilities in the mixing region of solar wind and Martian ionospheric plasma (Dubinin et al. 2013). At 600 km, during May 10 the peak flux shifted to higher energies where ion pickup is dominating the energization process. The SIR/HSS acts as a pressure pulse within the solar wind, thereby increasing the solar wind forcing on the planetary ionosphere. This increased solar wind dynamic pressure and IMF can lead to intense particle precipitation and enhanced motional electric field within the planetary ionosphere, leading to an increase in ion energization (Krishnaprasad et al. 2019). The results indicate an increased heavy ion energization in the Martian dayside ionosphere due to enhanced solar wind interaction during the SIR/HSS passage.

It was noticed that on Earth, the enhancement occurred mainly on May 8, but on Mars, it lasted for more than one day (May 9 and 10). This extended duration on Mars could be attributed to the direct interaction of the Martian ionosphere with the solar wind, which allows the effects of the disturbed solar wind and subsequent energization of ions to last longer compared to that on Earth. The ion energization mechanisms on Earth are found to be mostly indirect compared to that on Mars. Dynamic pressure leads to the compression of the Earth's magnetosphere, which in turn increases the ambipolar diffusion at the poles. Similarly, the nightside energetic electrons are mostly accelerated within the magnetosphere as they travel from the tail to the high-latitude ionosphere. Also, these outflowing ions are not completely out of the influence of the Earth. They remain trapped within the Earth's magnetosphere or escape completely based on their trajectory and energy within the magnetosphere. In the case of Mars, increased solar wind ion flux is seen at the points of increased ion energization which indicates direct solar wind interaction and energization at Mars. Therefore, the SIR/HSS passage enhanced the O^+ ion outflow from both Earth and Mars, but the differing magnetic behaviors of the planets

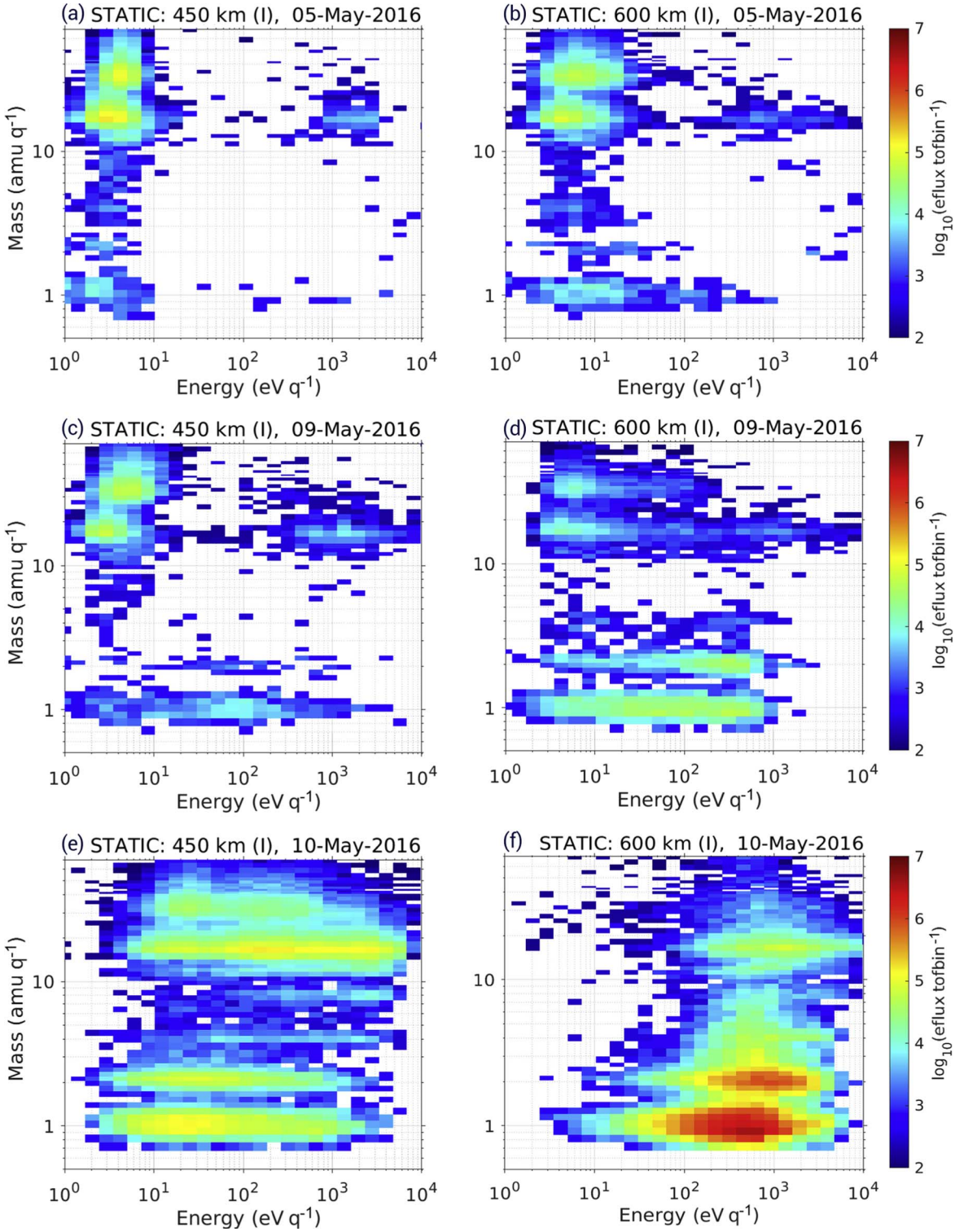

Figure 7. The STATIC measurements at 450 and 600 km altitude. (a) and (b) May 5—periapsis 1, (c) and (d) May 9—periapsis 4, (e) and (f) May 10—periapsis 2. The unit of eflux is $\frac{\text{eV}}{\text{eV cm}^2\,\text{s sr}}$.

led to differences in the duration and energization mechanisms of the ion outflow. However, it should be noted that though this study showcases the differences in processes that drive the ion outflows, the calculation of global atmospheric escape rates of Earth and Mars is not straightforward, given the complexity of these escape mechanisms and different boundary conditions.

5. Conclusion

In the present study, we have analyzed the O^+ ion outflows at Earth and Mars during the passage of an SIR/HSS, when Sun, Earth, and Mars were nearly aligned. We observed enhanced ion outflows on both planets caused by the passage of SIR/HSS. On Earth, direct ion outflow from the high-latitude ionosphere into

the inner magnetosphere was observed by Van Allen probes on the dayside, while the MMS satellite was located in the nightside. Major ion outflow triggers identified for Earth are the solar wind dynamic pressure and strong upward FAC, generated during the geomagnetic storm caused during the SIR/HSS passage. In the case of Mars, during the event periods, solar wind was able to penetrate deeper into the ionosphere due to increased dynamic pressure and IMF associated with the SIR/HSS. Increased solar wind interaction thus facilitated stronger ion energization through particle precipitation, ion–ion instabilities, and ion pickup mechanisms. The results suggest that even though Earth has an intrinsic magnetic field that considerably reduces the direct solar wind interaction with the planetary ionosphere, energy from the solar wind is channeled to the ionosphere in various ways triggering ion outflow. Therefore, ion outflow from Earth is a more localized process compared to Mars with an induced magnetosphere.

Acknowledgments

The work is supported by the Indian Space Research Organization. The MAVEN/STATIC ion energy flux data (Level 2, Version 2, Revision 0) used in this work is obtained from the NASA Planetary Data System (https://pds.nasa.gov/). We thank the MAVEN team for the data. The MEX data are obtained from AMDA database (http://amda.cdpp.eu). We gratefully acknowledge the AMDA team for the data. The WIND/ACE data are taken from the OMNIweb database (https://omniweb.gsfc.nasa.gov/). We thank the OMNIweb team for the data. The Van Allen Probes/HOPE instrument data used in this study are publicly available on the website RBSP-ECT Science Operations and Data Centre (https://rbsp-ect.newmexicoconsortium.org/data_pub/rbspa/hope/level3/). We thank the Van Allen Probe team for the data. The MMS/HPCA data are obtained from the MMS Science Data Centre (https://lasp.colorado.edu/mms/sdc/public/). We thank the MMS team for the data. The pyspedas package is used for visualizing the MMS data. We thank the pyspedas community. I.V. acknowledges the financial assistance provided by ISRO through a research fellowship.

ORCID iDs

Indu Venugopal https://orcid.org/0009-0006-5587-1868
Smitha V. Thampi https://orcid.org/0000-0002-0116-829X
Ankush Bhaskar https://orcid.org/0000-0003-4281-1744
V. Venkataraman https://orcid.org/0000-0001-8093-007X

References

Besliu-Ionescu, D., Maris Muntean, G., & Dobrica, V. 2022, SoPh, 297, 65
Cai, L., Aikio, A., Kullen, A., et al. 2022, FrASS, 9, 387
Caggiano, J., & Paty, C. S. 2022, JGRA, 127, e2021JA029414
Cully, C. M., Donovan, E. F., Yau, A. W., & Arkos, G. G. 2003, JGRA, 108, 1093
Dandouras, I. 2021, JGRA, 126, e2021JA029753
Dieval, C. 2011, PhD thesis, Luleå Univ. of Technology
Dubinin, E., Fraenz, M., Zhang, T., et al. 2013, JGRA, 118, 7624
Fernandes, P. A., Larsen, B. A., Thomsen, M. F., et al. 2017, JGRA, 122, 9207
Fowler, C. M., Ergun, R. E., Andersson, L., et al. 2017, JGRA, 122, 10612
Funsten, H., Skoug, R., Guthrie, A., et al. 2013, SSRv, 179, 423
Fuselier, S. A., Collin, H. L., Ghielmetti, A. G., et al. 2002, JGRA, 107, 1203
Fuselier, S. A., Klumpar, D. M., Peterson, W. K., & Shelley, E. G. 1989, GeoRL, 16, 1121
Gkioulidou, M., Ohtani, S., Ukhorskiy, A. Y., et al. 2019, JGRA, 124, 405
Gruesbeck, J., Espley, J., Lee, C., & Curry, S. 2021, JGRA, 126, e2021JA029479
Hall, B. E. S., Sánchez-Cano, B., Wild, J. A., Lester, M., & Holmström, M. 2019, JGRA, 124, 4761
Harada, Y., Halekas, J., McFadden, J., et al. 2015, GeoRL, 42, 8925
Jakosky, B. M., Grebowsky, J. M., Luhmann, J. G., & Brain, D. A. 2015, GeoRL, 42, 8791
Jakosky, B. M., Lin, R. P., Grebowsky, J. M., et al. 2015, SSRv, 195, 3
Kistler, L. M., Mouikis, C. G., Asamura, K., et al. 2019, JGRA, 124, 10036
Krishnaprasad, C., Thampi, S. V., & Bhardwaj, A. 2019, JGRA, 124, 6998
Li, S., Lu, H., Cao, J., et al. 2023, ApJ, 949, 88
Liu, Z. Y., & Zong, Q. G. 2022, JGRA, 127, e2022JA030611
Lundin, R., Barabash, S., Andersson, H., et al. 2004, Sci, 305, 1933
Lundin, R., Barabash, S., Fedorov, A., et al. 2008, GeoRL, 35, L09203
Lundin, R., Winningham, D., Barabash, S., et al. 2006, Icar, 182, 308
Karoly, S. 2012, The Plasma Environment of Venus, Mars, and Titan (New York: Springer)
Madanian, H., Hesse, T., Duru, F., Pilinski, M., & Frahm, R. 2024, AnGeo, 42, 69
McFadden, J., Kortmann, O., Curtis, D., et al. 2015, SSRv, 195, 199
McFadden, J. P. 2024, MAVEN STATIC Calibrated Energy Flux: 32 Energy X 64 Mass Bins Data Collection, NASA Planetary Data System, doi:10.17189/1517746
Nilsson, H., Zhang, Q., Wieser, G. S., et al. 2023, Icar, 393, 114610
Papitashvili, N. E., & King, J. H. 2020, OMNI 5-min Data Set, NASA Space Physics Data Facility, doi:10.48322/gbpg-5r77
Schillings, A. 2019, PhD thesis, Luleå Univ. of Technology
Seki, K., Elphic, R. C., Hirahara, M., Terasawa, T., & Mukai, T. 2001, Sci, 291, 1939
Strangeway, R., Ergun, R., Su, Y.-J., Carlson, C., & Elphic, R. 2005, JGRA, 110, A03221,
Thampi, S. V., Krishnaprasad, C., Bhardwaj, A., et al. 2018, JGRA, 123, 6917
Wei, Y., Fraenz, M., Dubinin, E., et al. 2012, JGRA, 117, A03208
Young, D., Burch, J., Gomez, R., et al. 2016, SSRv, 199, 407
Zhang, Q. 2023, PhD thesis, Umeå Univ.